

UNCLASSIFIED

AD NUMBER

AD907161

LIMITATION CHANGES

TO:

Approved for public release; distribution is unlimited.

FROM:

Distribution authorized to U.S. Gov't. agencies only; Test and Evaluation; 07 FEB 1973. Other requests shall be referred to Ballistic Research Laboratories, ATTN; AMXBR-XSE, Aberdeen Proving Ground, MD 21005.

AUTHORITY

USABRL per ltr, 13 Nov 1986

THIS PAGE IS UNCLASSIFIED

AD 907 161

AUTHORITY:

BRL etc.,

13 NOV 86



THIS REPORT HAS BEEN DELIMITED  
AND CLEARED FOR PUBLIC RELEASE  
UNDER DOD DIRECTIVE 5200.20 AND  
NO RESTRICTIONS ARE IMPOSED UPON  
ITS USE AND DISCLOSURE.

DISTRIBUTION STATEMENT A

APPROVED FOR PUBLIC RELEASE;  
DISTRIBUTION UNLIMITED.

AD907161

BRLR 1620

# BRL

AD

REPORT NO. 1620

THEORY AND COMPUTATIONS OF  
COLLAPSE AND JET VELOCITIES OF  
METALLIC SHAPED CHARGE LINERS

by

A. R. Kiwan  
H. Wisniewski

November 1972



7 FEB 1973

"TEST + EVALUATION"

Distribution limited to US Government agencies only.  
Other requests for this document must be referred to  
Director, USA Ballistic Research Laboratories, ATTN:  
AMXBR-XSE, Aberdeen Proving Ground, Maryland 21005.

USA BALLISTIC RESEARCH LABORATORIES  
ABERDEEN PROVING GROUND, MARYLAND

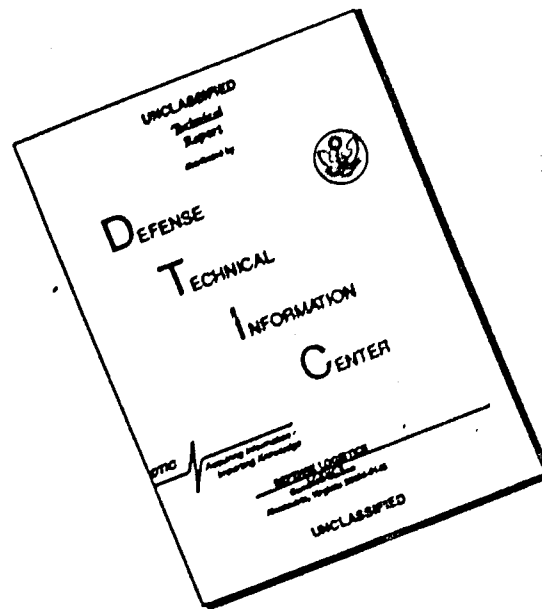
Destroy this report when it is no longer needed.  
Do not return it to the originator.

Secondary distribution of this report by originating or  
sponsoring activity is prohibited.

Additional copies of this report may be purchased from  
the U.S. Department of Commerce, National Technical  
Information Service, Springfield, Virginia 22151

The findings in this report are not to be construed as  
an official Department of the Army position, unless  
so designated by other authorized documents.

# DISCLAIMER NOTICE



THIS DOCUMENT IS BEST QUALITY AVAILABLE. THE COPY FURNISHED TO DTIC CONTAINED A SIGNIFICANT NUMBER OF PAGES WHICH DO NOT REPRODUCE LEGIBLY.

BALLISTIC RESEARCH LABORATORIES

REPORT NO. 1620

NOVEMBER 1972

THEORY AND COMPUTATIONS OF COLLAPSE  
AND JET VELOCITIES OF METALLIC SHAPED CHARGE LINERS

A. R. KIWAN  
H. WISNIEWSKI

TERMINAL BALLISTICS LABORATORY

"TEST + EVALUATION"

Distribution limited to US Government agencies only.  
Other requests for this document must be referred to  
Director, USA Ballistic Research Laboratories, ATTN:  
AMABR-XSE, Aberdeen Proving Ground, Maryland 21005.

RDT&E Project No. 1T0061102A33E

ABERDEEN PROVING GROUND, MARYLAND

BALLISTIC RESEARCH LABORATORIES

REPORT NO. 1620

ARKiwan HWisniewski/ng  
Aberdeen Proving Ground, Md.  
November 1972

THEORY AND COMPUTATIONS OF COLLAPSE  
AND JET VELOCITIES OF METALLIC SHAPED CHARGE LINERS

ABSTRACT

A model to compute the collapse velocities of various elements of a metallic liner of a shaped charge from the known detonation properties of the explosive used and the geometrical configurations of the charge is proposed. The calculated collapse and jet velocities increase from the apex of the liner toward the base, reach a maximum, and then decrease monotonically thereafter. The calculated velocity distribution in the jet after it goes through compression agrees qualitatively and quantitatively with available experimental measurements.



## TABLE OF CONTENTS

	Page
ABSTRACT. . . . .	3
LIST OF SYMBOLS . . . . .	7
I. INTRODUCTION. . . . .	9
II. PRESSURE APPROXIMATION. . . . .	11
III. NUMERICAL INTEGRATION OF THE EQUATIONS OF MOTION. . . . .	14
IV. APPLICATION . . . . .	21
REFERENCES. . . . .	24
DISTRIBUTION LIST . . . . .	33

# LIST OF SYMBOLS

$x, y, z$	Eulerian Coordinates
$t$	time variable
$p$	pressure
$p_f$	pressure at the detonation front
$p_o$	ambient atmosphere pressure
$I$	impulse
$u$	particle velocity in the pressure wave
$c$	sound speed in the pressure wave
$U$	detonation velocity
$2k$	the height of the charge
$2\ell$	the thickness of the charge
$\alpha$	half angle of the charge liner
$n$	number of liner zones
$\beta$	half angle of collapsing liner
$\delta m^k$	the $k^{th}$ element of liner mass
$\delta m_j^k$	the mass of the $k^{th}$ jet element
$\delta m_g^k$	the mass of the $k^{th}$ slug element
$\overline{uc}$	average value of $(u+c)$ over the pressure wave
$v_j^k, v_j^k$	velocities of $k^{th}$ liner jet element relative to stationary and moving coordinate systems
$v_g^k, v_g^k$	velocities of $k^{th}$ liner slug element relative to stationary and moving coordinate systems.
$e$	coefficient of restitution

## I. INTRODUCTION

The existing theory of explosives with metallic lined cavities was first published in the open literature in 1948 by Birkhoff, MacDougall, Pugh and Taylor [1]\*. The paper gave a qualitative description of the phenomenon of collapse of a metallic liner of a shaped charge and the formation of a jet. The quantitative part of the theory provided a first order approximation to the various characteristics of the phenomenon. The whole theory was based on simulating the relative motion of the metallic liner during collapse with the steady flow of two jets of water impinging upon each other as developed by Milne-Thomson in [2]. The relative motion considered here is with respect to an observer at the stagnation point. The theory assumed that each element of the liner collapses with a constant velocity  $V_0$ , and thus the ensuing jet was a uniform one of a constant length  $l$ , equal to the length of the side of the uncollapsed liner, and had a uniform distribution of velocity along it. Pugh, Eichelberger and Rostoker [3] modified the earlier theory by assuming the velocity of collapse  $V_0$  to be a function of position on the liner which decreases monotonically from apex to base. This modification had the effect of elongating the ensuing jet and producing a velocity gradient along its length. An enormous amount of literature has appeared since then which is mostly of an experimental nature and expounds the various aspects of the theory of shaped charges. In 1955 R. J. Eichelberger re-examined the non-steady theory of jet formation [4] and in his conclusion raised some doubts about the hydrodynamical model. Moreover, the theory, as developed in [1] and modified in [3], fails to correlate the velocity of collapse of a liner element to the properties of the explosive used, or to the

---

\*References are listed on page 24

geometrical configuration of the charge in question. The application of the theory as developed in [1] and [3], necessitated the experimental measurement of collapse velocities of various elements of a liner for each charge with a specified explosive and a given geometry.

The present paper takes into account the varying properties of various explosives and the different geometrical configurations of various charges and predicts quantitatively the collapse velocities of the various elements of a liner and the subsequent formation of a jet. The main ideas in the current investigation are the following:

1. The liner is replaced by a system of discrete solid liner elements. We assume that we may neglect forces of interaction between liner elements and strength properties of liner material. This is justified since the pressure at the detonation front is several orders of magnitude greater than the ultimate tensile strength of a typical liner material e.g. the peak pressure at the detonation front for pentolite at  $1.65 \text{ gm/cm}^3$  density is approximately  $2389.55 \text{ Kg/mm}^2$  (see [5]) while the ultimate tensile strength for quenched copper aluminum is  $85.40 \text{ Kg./mm}^2$ .

2. The impulse transmitted by the detonation products to a liner element is obtained by integrating the excess pressure  $p(x,y,t)$  along the path of the liner element. Thus if

$$x=x^k(t) \quad y=y^k(t) \quad (1.1)$$

are the parametric equations of the path of a typical liner element, then

$$I^k = \int_{t_0}^{t_s^k} p(x^k(t), y^k(t), t) dt, \quad (k=1, 2, \dots, n) \quad (1.2)$$

represents the total impulse per unit area of liner given to the  $k^{\text{th}}$  element by the time it reaches its stagnation point, where  $p(x,y,t)$  is the excess pressure over the atmosphere at the point  $(x,y)$  and time  $t$ ,  $t_0^k$  the instant the detonation front reaches the  $k^{\text{th}}$  element,  $t_s^k$  is the stagnation time of the same element and  $k$  is a Lagrangian coordinate indicating the initial position of the element. Flow properties behind the detonation front in T.N.T. were studied by Sir G. I. Taylor [6] and similar studies for pentolite were performed by R. Shear [5]. In this paper we shall restrict our considerations to wedge shaped liners Figure 1.

## II. PRESSURE APPROXIMATION

In this section we obtain an approximation to the pressure wave behind the detonation front in a shaped charge warhead. The starting point is the Taylor wave [6]. The pressure wave in the detonation products behind the front is approximated in the space  $(p, x/Ut)$  by a triangular pressure pulse. The variables  $p$ ,  $U$ ,  $t$ , and  $x$  denote the overpressure, the detonation velocity, the time measured from initiation, and the abscissa of the point under consideration. Let the origin of our stationary coordinate system be at the center of the plane of initiation of the charge as shown in Figure 1. We consider the function

$$p(Z) = p_f - p_0 + (p_f - p_0) (Z-1)/(1-\lambda_0), \quad \lambda_0 \leq Z \leq 1 \quad (2.1)$$

where,  $Z=x/Ut$ ,  $p_f$  the detonation pressure,  $p_0$  the ambient atmospheric pressure, to be an approximation to the overpressure distribution in a completely confined charge which has its initiation end open. Equivalently  $p(Z)$  is considered as an approximation to the one dimensional plane Taylor wave in a tube with an open end. The parameter  $\lambda_0$  in Equation (2.1) is the value of  $Z$  for which the part-

icle velocity  $u$  vanishes in the Taylor wave. The overpressure  $p(Z)$  as given by Equation (2.1) is modified whenever the charge is unconfined, and secondly it has to be modified further due to the presence of the cavity in the explosive which causes a reduction in the total available energy greater than otherwise assumed. For an unconfined charge the parameter  $\lambda_0$  in Equation (2.1), which determines the slope of the linear fit to the Taylor wave is replaced by  $\lambda_1$  where,

$$\lambda_1 = \lambda_0 + (1-\lambda_0) \left\{ \sum_{S_i} \delta A \left( 1 - \frac{l_n}{l_{uc}} \right) H(t - t_{\delta A}^0) \cdot H\left(1 - \frac{l_n}{l_{uc}}\right) \right\} / A_t. \quad (2.2)$$

In Equation (2.2),  $\delta A$  is an element of area of an unconfined surface  $S_i$  of the charge,  $\frac{l_n}{l_{uc}}(t)$  the distance traveled by the sound wave propagating from  $\delta A$  inward normal to the plane  $z = 0$  at time  $t$ ,  $l_n$  is the total distance along that normal from  $\delta A$  to the plane  $z = 0$ ,  $t_{\delta A}^0$  is the time of arrival of the detonation front at the element  $\delta A$ ,  $A_t$  is the total surface area of the charge up to the detonation front,  $\frac{l_n}{l_{uc}}$  is the average value of  $(u + c)$  over the wave as it sweeps over  $\delta A$ ,  $u$  is the particle velocity,  $c$  is the sound speed in the wave, and  $H(x)$  is the Heaviside step function. The summation in (2.2) is carried out over all unconfined surfaces  $S_i$  of the charge. Effectively Equation (2.2) accounts for the lack of confinement on the charge surface by increasing the slope of the linear fit to the pressure wave in the plane  $(p, x/Ut)$ , thus causing faster pressure decay. The contribution from an unconfined surface element  $\delta A$  is seen from equation (2.2) to be  $(1-\lambda_0) \delta A (1 - \frac{l_n}{l_{uc}}) / A_t$ , and its effect is felt only after the disturbance from  $\delta A$  has reached the plane  $z=0$  by virtue of  $H(1 - \frac{l_n}{l_{uc}})$ . Let  $E_i$ ,  $i = 1, 2, 3, 4$ , be a confinement function associated with surface  $S_i$  of the charge where,

$$E_i = 0 \text{ if } S_i \text{ is confined.}$$

$$E_i = 1 \text{ if } S_i \text{ is unconfined.}$$

Writing equation (2.2) in integral form one obtains

$$\lambda_1 = \lambda_0 + (1 - \lambda_0) \{ (E_1 + E_3) I_1 + (E_2 + E_4) I_2 \} / 4 (K + l) U t, \quad (2.3)$$

where

$$I_1 = \int_0^{U t} 2K [1 - l / \{\overline{uc} (t - x/U)\}] H(t - x/U) \cdot H(1 - l / \{\overline{uc} (t - x/U)\}) dx, \\ I_2 = \int_0^{U t} 4dx \int_0^l \{1 - z / \overline{uc} (t - x/U)\} H(t - x/U) \cdot H\{1 - z / \overline{uc} (t - x/U)\} dz. \quad (2.4)$$

Evaluating the integrals  $I_1$  and  $I_2$  and substituting in (2.3) one obtains

$$\lambda_1 = \lambda_0 + (1 - \lambda_0) N / 4 (K + l) U t \quad (2.5)$$

where,

$$N = \{ 2(E_1 + E_3) KU [ (t - l / \overline{uc}) + (l / \overline{uc}) \ln (l / \overline{uc} \cdot t) ] + 2(E_2 + E_4) \\ U l [ 2t - 3l / 2 \overline{uc} + (l / \overline{uc}) \cdot \ln (l / \overline{uc} \cdot t) ] \} H(t - l / \overline{uc}),$$

where,

$$\overline{uc} = \text{av} (u + c) = \text{av} \frac{(u + c)t}{U t} \cdot U = \text{av} \frac{x}{R} \cdot U = \text{av} Z \cdot U = U (1 + \lambda_0) / 2. \quad (2.6)$$

Equation (2.1) would thus be replaced by

$$p(Z) = p_f - p_0 + (p_f - p_0) (Z - 1) / (1 - \lambda_1). \quad (2.7)$$

The overpressure distribution as given by (2.7) needs one further

modification due to the presence of the cavity in the explosive and hence the loss of available energy. This modification is effected as before by increasing the slope of our linear fit. Equation (2.7) is modified to

$$p(Z) = p_f - p_o + (p_f - p_o) (Z - 1) / [1 - \{\lambda_1 + (1 - \lambda_1) V_c / V_t\}], (2.8)$$

where  $V_c$  is the volume of the cavity up to the detonation front,  $V_t$  is the total volume of the explosive which would have been present from the apex of the liner up to the detonation front had the cavity been absent.  $V_c$  and  $V_t$  are given by

$$V_c = 2\ell (Ut-d)^2 \tan \alpha \cdot H(t - t_o^1)$$

$$V_t = 4\ell K [(Ut-d) H(t_o^n - t) + (U t_o^n - d) H(t - t_o^n)].$$

Equation (2.8) then reduces to

$$p(x,y,t) = p_f - p_o + (p_f - p_o) (x/Ut - 1) / [1 - \{\lambda_1 + (1 - \lambda_1) (Ut-d)^2 \tan \alpha \cdot H(t - t_o^1) / 2K [(Ut-d) H(t_o^n - t) + (U t_o^n - d) H(t - t_o^n)]\}]. (2.9)$$

Equation (2.9) reveals our assumption of plane detonation wave in the fact that  $p$  is independent of  $y$  and  $z$  and is a function of  $x$  and  $t$  only. Figure 2 shows a schematic of a cross section of the charge, and Figure 3 shows the triangular wave profile for charge 5 at different times measured from initiation.

### III. NUMERICAL INTEGRATION OF THE EQUATIONS OF MOTION

For each strip of the liner we integrate numerically the following set of equations which are obtained from Newton's laws of motion



$$\sigma \dot{x}^k = p(x^k(t), y^k(t), t) \cdot \sin \alpha \quad (3.1)$$

$$\sigma \dot{y}^k = -p(x^k(t), y^k(t), t) \cdot \cos \alpha \quad (3.2)$$

$k = 1, 2, \dots, n$ , where  $p(x, y, t)$  is given by (2.9),  $\sigma$  is the mass per unit area of the liner and the dot indicates differentiation with respect to  $t$ . This implicitly involves the assumption that each element of the liner collapses in a direction perpendicular to the surface of its initial position on the liner. This assumption is consistent with assuming the flow in the detonation products to be inviscid and was made earlier by G. Birkhoff [7]. The integration of (3.1), (3.2) is carried out subject to the conditions:

$$\text{at } t = t_0^k; x^k = x_0^k = d + h(2k-1)/2n, \dot{x}^k = 0$$

$$y^k = y_0^k = h \tan \alpha (2k-1)/2n, \dot{y}^k = 0 \quad (3.3)$$

$$\text{and} \quad t_0^k = x_0^k / U \quad k=0, 1, 2, \dots, n \quad (3.4)$$

The numerical integration of (3.1), (3.2) is terminated at  $t_1^k$  which is such that

$$P(x^k, y^k, t_1^k) = 0 \quad (3.5)$$

or at  $t_s^k$  which satisfies (see Fig. 3)

$$y^k(t_s^k) = 0. \quad (3.6)$$

In the case of  $t_1^k < t_s^k$ , the motion of the  $k^{\text{th}}$  element for  $t_1^k < t < t_s^k$  is given by

$$x^k = x_1^k + (t - t_1^k) \dot{x}_1^k \quad (3.7)$$

$$y^k = y_1^k + (t - t_1^k) \dot{y}_1^k \quad (3.8)$$

where  $x_1^k, y_1^k, \dot{x}_1^k, \dot{y}_1^k$  are the coordinates and the velocity components of the  $k^{\text{th}}$  element at  $t = t_1^k$ . The stagnation time  $t_s^k$  is obtained in this case by setting in (3.8)

$$y^k = 0$$

$$\text{i.e.} \quad t_s^k = t_1^k - y_1^k / \dot{y}_1^k \quad (3.9)$$

and the stagnation point in this case

$$x_s^k = x_1^k - \dot{x}_1^k \cdot y_1^k / \dot{y}_1^k \quad (3.10)$$

The velocity of collapse at the stagnation point is given in this case by

$$v_p^k = \left\{ (\dot{x}_1^k)^2 + (\dot{y}_1^k)^2 \right\}^{1/2} \quad (3.11)$$

In the other case of  $t_s^k < t_1^k$ , i.e., when the particle reaches the axis before the overpressure vanishes,

$$v_p^k = \left\{ (\dot{x}_s^k)^2 + (\dot{y}_s^k)^2 \right\}^{1/2} \quad (3.12)$$

Combining Equations (3.1), (3.2) one obtains

$$\ddot{x}^k + \tan \alpha \cdot \dot{y}^k = 0. \quad (3.13)$$

Integrating (3.13) subject to (3.3) one arrives at

$$\dot{x}^k + \tan \alpha \cdot \dot{y}^k = 0$$

$$y^k = (d - x^k) \cdot \cot \alpha + 2h(2k-1)/2n \sin 2\alpha \quad (3.14)$$

This is the equation of the trajectory of the  $k^{\text{th}}$  particle. Setting  $y^k = 0$  in Equation (3.14) one obtains

$$x_s^k = d + h \sec^2 \alpha (2k-1)/2n \quad (3.15)$$

Equation (3.15) may be used to check the numerical integration.

When the  $k^{\text{th}}$  particle reaches the stagnation point, the distribution of velocities is as shown in Figure 4, where  $\vec{V}_p^k$  is the actual velocity of the  $k^{\text{th}}$  particle relative to our fixed coordinate system as it enters the stagnation point.  $\vec{V}_s^k$  is the velocity of the stagnation point, relative to the fixed axes as the  $k^{\text{th}}$  particle enters it, and

$$\vec{V}_r^k = \vec{V}_p^k - \vec{V}_s^k \quad (3.16)$$

is the velocity of the  $k^{\text{th}}$  particle relative to the stagnation point. Since  $\vec{V}_p^k$  has been determined above it remains to determine  $\vec{V}_s^k$ ,  $\beta^k$  and

$\vec{V}_r^k$ .  $|\vec{V}_s^k|$  is determined numerically, thus

$$V_s^k(t_s^k) \approx (x_s^{k+1} - x_s^{k-1}) / (t_s^{k+1} - t_s^{k-1}).$$

Using Equation (3.15) this reduces to

$$V_s^k(t_s^k) \approx 2h \sec^2 \alpha / n (t_s^{k+1} - t_s^{k-1}) \quad (k=1, 2, \dots, n). \quad (3.17)$$

$t_s^1, t_s^2, \dots, t_s^n$  are obtained above in the numerical integration,

$$t_s^0 = (d - h \sec^2 \alpha / 2n) / U$$

by definition and  $t_s^{n+1}$  is obtained by quadratic extrapolation i.e.,

$$t_s^{n+1} = a(n+1)^2 + b(n+1) + c, \quad (3.18)$$

where ,

$$a = [t_s^n - 2t_s^{n-1} + t_s^{n-2}] / 2$$

$$b = (3-2n)t_s^n/2 + 2(n-1)t_s^{n-1} - (3n-1)t_s^{n-2}/2$$

$$\text{and } c = (n-1)(n-2)t_s^n/2 - n(n-2)t_s^{n-1} + n(n-1)t_s^{n-2}/2.$$

From Figure 4

$$|\vec{v}_r^k| / \cos \alpha = |\vec{v}_p^k| / \sin \beta^k = |\vec{v}_s^k| / \sin(\pi/2 + \alpha - \beta^k) \quad (3.19)$$

and hence

$$\cot \beta^k = |\vec{v}_s^k| \cdot \sec \alpha / |\vec{v}_p^k| - \tan \alpha$$

$$\text{i.e. } \cot \beta^k = |\vec{v}_s^k| / |\dot{y}_s^k| - \tan \alpha \quad (3.20)$$

and hence  $\beta^k$  may be evaluated. At the stagnation point the  $k^{\text{th}}$  particle  $\delta m^k$  is divided into two parts  $\delta m_j^k$  and  $\delta m_g^k$  and we have by the laws of conservation of mass and momentum

$$\delta m^k = \delta m_j^k + \delta m_g^k \quad (3.21)$$

$$-\delta m^k \cdot |\vec{v}_r^k| \cos \beta^k = \delta m_j^k \cdot v_j^k + \delta m_g^k \cdot v_g^k \quad (3.22)$$

where  $v_j^k$  and  $v_g^k$  are the velocities of  $\delta m_j^k$  and  $\delta m_g^k$  relative to an observer at the stagnation point. An observer stationed at the stagnation point will observe the flow of the liner material to be nonsteady, however for the sake of simplicity we shall assume that

$$v_g^k = - |\vec{v}_r^k| = - v_j^k. \quad (3.23)$$

Equation (3.23) amounts to assuming the flow of liner material relative to the stagnation point to be steady and that the law of conservation

of energy holds there. It is to be observed that equation (3.23) was first used by G. Birkhoff, D. P. MacDougall, E. M. Pugh and Sir G. I. Taylor in [1] and later by E. M. Pugh, R. J. Eichelberger and N. Rostoker [3]. Using (3.23) in (3.22) and then solving (3.21), (3.22) one obtains the familiar results

$$\delta m_j^k / \delta m^k = \sin^2(\beta^k/2) \quad (3.24)$$

$$\delta m_g^k / \delta m^k = \cos^2(\beta^k/2) \quad (3.25)$$

If  $\vec{V}_j^k$  and  $\vec{V}_g^k$  are the respective velocities of  $\delta m_j^k$  and  $\delta m_g^k$  relative to fixed coordinate axes as they leave the stagnation point then

$$|\vec{V}_j^k| = |\vec{V}_s^k + \vec{V}_j^k| = |\vec{V}_s^k| + |\vec{V}_r^k| \quad (3.26)$$

$$|\vec{V}_g^k| = |\vec{V}_s^k + \vec{V}_g^k| = |\vec{V}_s^k| - |\vec{V}_r^k|. \quad (3.27)$$

Substituting for  $V_s^k$  and  $|\vec{V}_r^k|$  their values from (3.19) one obtains

$$|\vec{V}_j^k| = |\vec{V}_p^k| \cos(\alpha - \beta^k/2) / \sin(\beta^k/2) \quad (3.28)$$

$$|\vec{V}_g^k| = |\vec{V}_p^k| \sin(\alpha - \beta^k/2) / \cos(\beta^k/2) \quad (3.29)$$

Equations (3.28) and (3.29) agree with equations (5) and (6) of Pugh, Eichelberger and Rostoker [3] when one substitutes in the latter equations  $\delta = 0$ .

An examination of the computed jet velocity distribution when plotted as a function of its initial position (Lagrangian coordinate) on the liner reveals that this distribution cannot be stable. This instability is due to the presence of an inverse(positive) velocity gradient Figure 9. From a physical point of view this means that

as the various jet elements form and emerge from their stagnation points; the jet undergoes a continuous process of compression. During compression, momentum and energy are continuously transferred from the rear portion of the jet to the front portion until a physically stable velocity distribution is attained in the jet. A physically stable velocity distribution is one which has no inverse velocity gradient and in fact is what would be observed experimentally. This phenomenon of jet compression has been well known to experimenters for sometime. To simulate mathematically the process of jet compression, in its generality, is a rather complex task. The compression phase can be simulated in a simplified form, by treating it as the elastic collision of a string of heavy particles with the instantaneous mass and velocity distributions. Mathematically this is accomplished by an iterative procedure. Suppose the  $\ell^{\text{th}}$  liner element has already collapsed and reached its stagnation point and the jet underwent compression. Let the jet velocities at that stage be denoted by  $u^k$ ,  $k=1, \dots, \ell$ . As the  $(\ell+1)^{\text{th}}$  liner element collapses and reaches its stagnation point then we set  $u_0^k = u^k$ ,  $k=1, \dots, \ell$ , and  $u_0^{\ell+1} = V_j^{\ell+1}$ . For  $i=0, 1, 2, \dots$  one compares  $u_i^k$  and  $u_i^{k+1}$ , ( $k=1, 2, \dots, \ell$ ). If  $u_i^k < u_i^{k+1}$  then this means that particles  $k$  and  $(k+1)$  go through a collision process and acquire new velocities

$$u_{i+1}^k = [\delta m_j^k u_i^k + \delta m_j^{k+1} u_i^{k+1} - e \delta m_j^{k+1} (u_i^k - u_i^{k+1})] / [\delta m_j^k + \delta m_j^{k+1}] \quad (3.30)$$

$$(u_{i+1}^{k+1}) = [\delta m_j^k u_i^k + \delta m_j^{k+1} u_i^{k+1} + e \delta m_j^{k+1} (u_i^k - u_i^{k+1})] / [\delta m_j^k + \delta m_j^{k+1}], \quad (3.31)$$

otherwise the velocities of particles  $k$ ,  $(k+1)$  remain unchanged. Next we turn our considerations to particles  $(k+1)$  and  $(k+2)$  where the velocity of  $(k+1)$  is given by Equation (3.31). The  $i^{\text{th}}$  iteration is terminated when  $k$  assumes the values  $1, 2, \dots, \ell$ . The whole iteration process is terminated when the condition  $u_i^{k+1} \leq u_i^k$  is satisfied for all  $k=1, 2, \dots, \ell$ . Equations (3.30) and (3.31) are obtained by

solving the equations of conservation of momentum together with the equation defining the coefficient of restitution,  $e$  [8]. The parenthesis surrounding  $u_{i+1}^{k+1}$  in Equation (3.31) indicates that this velocity is not the final one for this iteration. The above iterative process is analogous to the Gauss-Seidel method.

#### IV. APPLICATION

The preceeding theory was applied to charges with geometry as shown in Figures 5 and 6 loaded with composition B with loading density  $1.7 \text{ gms/cm}^3$ . These charges are 4 inches thick. Figure 7 shows the collapse velocity curves of liner elements as functions of their initial positions. Figure 8 shows collapse angle curves and Figure 9 shows the jet velocity curves for the various liner elements as they emerge from their stagnation points. The dotted curves are the final jet velocity distributions after these jets go through a compression process. Two compression cases have been considered  $e=1$  (perfectly elastic), and  $e=0$  (perfectly inelastic), and are shown in Figure 9. Table 1 shows how the various computed properties of charge 5 vary as functions of the number of zones across the liner and hence is indicative of the speed of convergence. The velocity of the tip of the jet for charge 6 was found to be  $0.591 \text{ cms}/\mu \text{ sec}$ , ( $e=1$ ) and  $0.543 \text{ cms}/\mu \text{ sec}$  ( $e=0$ ), while the ratio of the liner's mass in the slug was found to be 0.79. The calculation reveals that the tip of the jet reaches its terminal velocity rather early in the collapse process, for example for charge 6 the tip of the jet ( $e=1$ ) reaches its terminal velocity after 0.09 of the liner had collapsed. R. Dipersio observed that the calculated slug velocity distributions for some cases reveals the existence of an inverse velocity gradient in the slug and indicates a compression process similar to that occurring in the jet. This phenomenon of slug compression is known experimentally.

TABLE 1

No. of Liner Zones	Percentage of Liner Mass in Slug	Velocity of Tip of Jet cm/ $\mu$ sec (e=1)	Velocity of tip of Jet cm/ $\mu$ sec (e=0)
10	0.856	0.714	0.706
20	0.863	0.732	0.691
30	0.865	0.737	0.688
40	0.866	0.741	0.686
50	0.866	0.743	0.685
100	0.867	0.746	0.684
200	0.867	0.747	0.684

The geometry and dimensions of charges 5 and 6 were taken from a report by Dipersio, Whiteford, and Simon[9]. The experimental scatter in the results given in [9] is rather large and prevents a precise comparison, although the calculation results are in agreement with accepted experimental values for such charges.

This model has a virtue of simplicity, does not need any experimental measurements for its utilization and can therefore be used for parametric study. Two computer codes exist with one difference between them. The first code performs the compression of the jet in real physical time while the second delays the compression until the whole collapse phenomenon is terminated. The second code is about twice as fast as the first code. The second code runs in about 3 to 4 minutes on BRLESC II for a case using 100 liner zones.

A possible future improvement for this model would result if one computes the pressure wave using a convenient hydro-code and then couple this calculation with the present code to predict the collapse and jet formation characteristics. The inclusion of strength properties



of the liner material might also be important in the collapse process near the base of the liner

#### ACKNOWLEDGMENTS

The work contained in this report was carried out in late 1968 upon the request of Mr. Julius Simon of TBL and Dr. C. Masaitis of AMD and was circulated internally in BRL as a report. My thanks are due to Mr. Richard Vitali, chief of the Warhead and Armor Branch, TBL, who renewed my interest in this problem and encouraged its publication in this report.

#### REFERENCES

- [1] G. Birkhoff, D. P. MacDougall, E. M. Pugh and Sir G. I. Taylor, "Explosives with Lined Cavities: J. Appl. Phys. 19 (1948) p. 563.
- [2] L. M. Milne - Thomson, "Theoretical Hydrodynamics" Macmillan London (1938) paragraph 11.43.
- [3] E. M. Pugh, R. J. Eichelberger and N. Rostoker, "Theory of Jet Formation by Charges with Lined Conical Cavities" J. Appl. Phys. 23 (1952) p. 532.
- [4] R. J. Eichelberger, "Re-Examination of the Nonsteady Theory of Jet Formation by Lined Cavity Charges" J. Appl. Phys. 26 (1955) p. 398.
- [5] R. E. Shear, "Detonation Properties of Pentolite" BRL Report No. 1159 (1961).
- [6] G. I. Taylor, "The Dynamic of Combustion Products Behind Plane and Spherical Detonation Fronts in Explosives" Proc. Royal Soc. 1950 V. 200 Series A.
- [7] G. Birkhoff, "Mathematical Jet Theory of Lined Hollow Charges" BRL Report No. 370 (1943).
- [8] H. M. Dadourian, Analytical Mechanics, D. Van Nostrand Company, New York (1931) page 316.
- [9] R. Dipersio, C. W. Whiteford and J. Simon, "An Experimental Method of Obtaining Collapse Velocities of the Inner Walls of a Linear Shaped-Charge Liner" BRL Memorandum Report No. 1696 (1965).

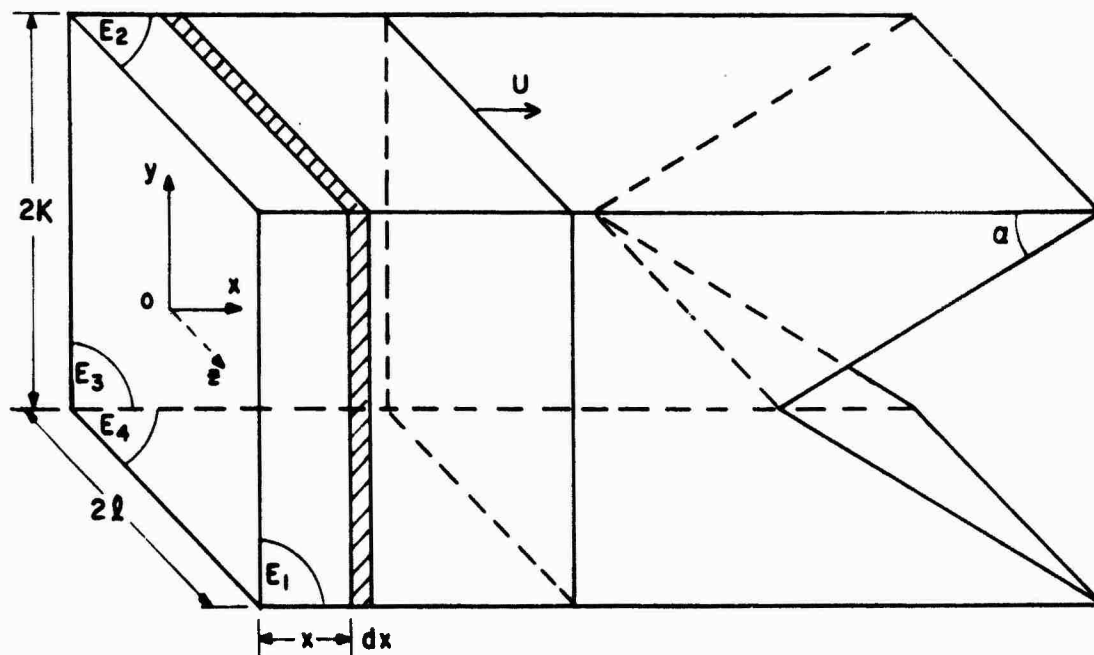


Figure 1. Schematic Drawing of a Typical Charge.

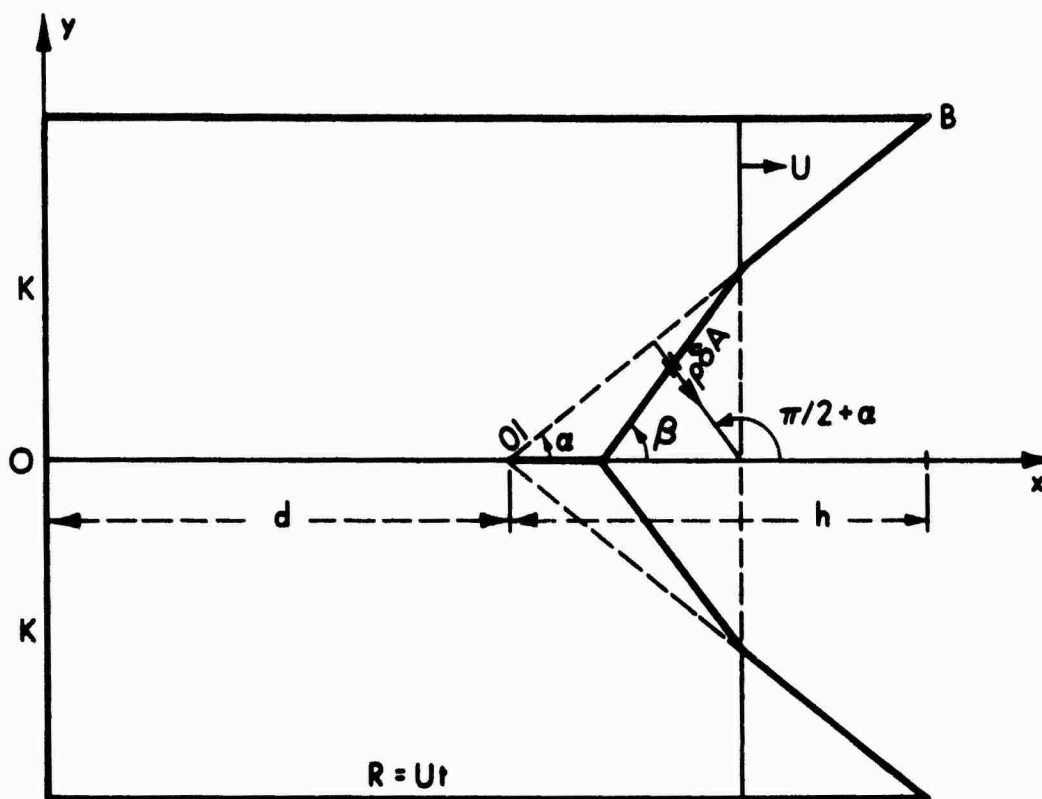


Figure 2. Schematic Representation of the Collapsing Liner.

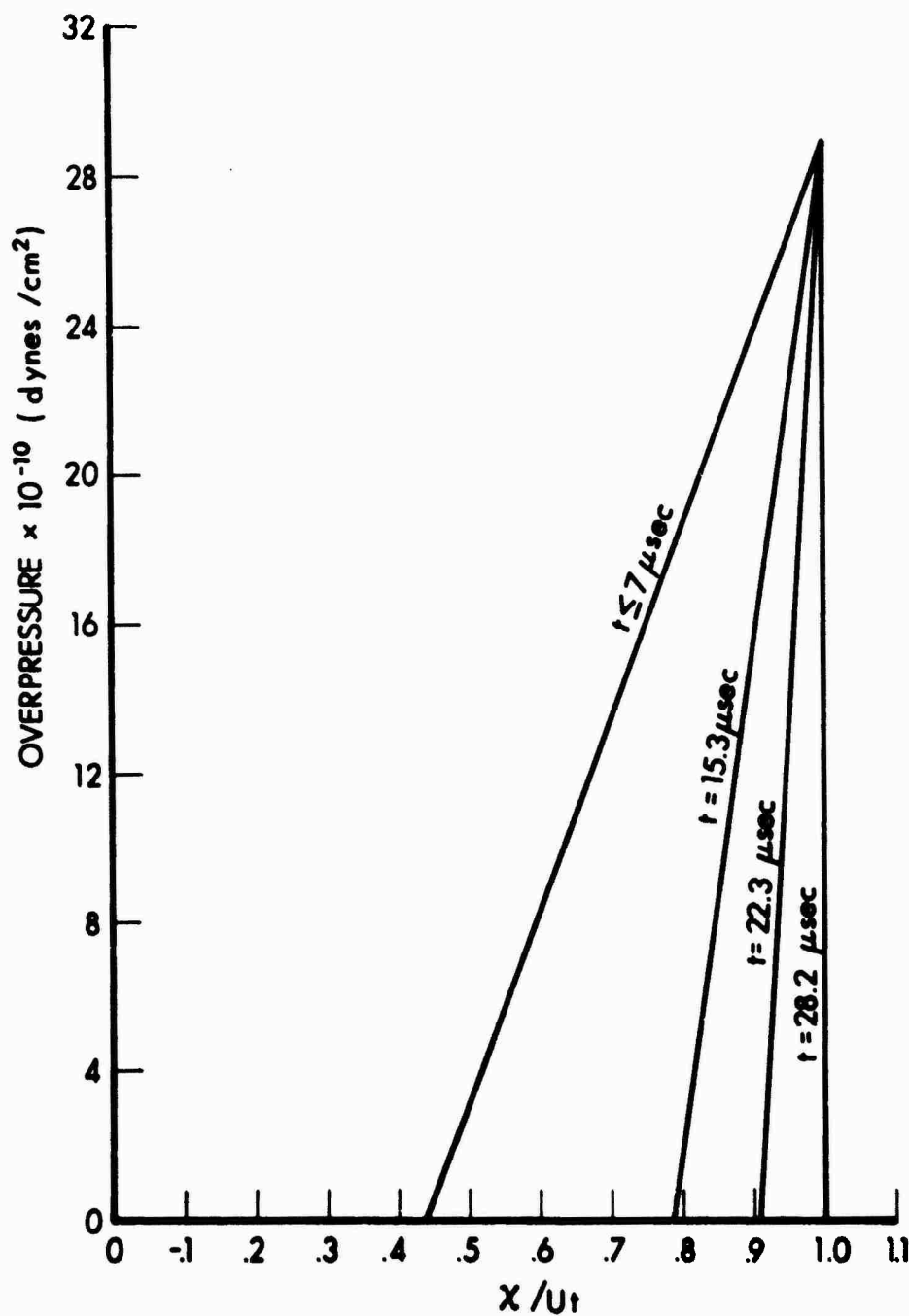


Figure 3. Profile of the Pressure Wave for Charge 5 at Various Times.

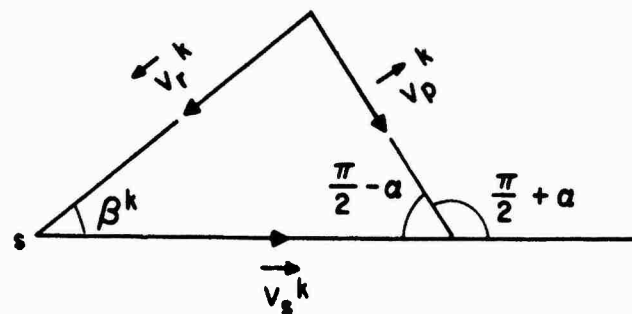


Figure 4. Distribution of Velocities at the Stagnation Point.

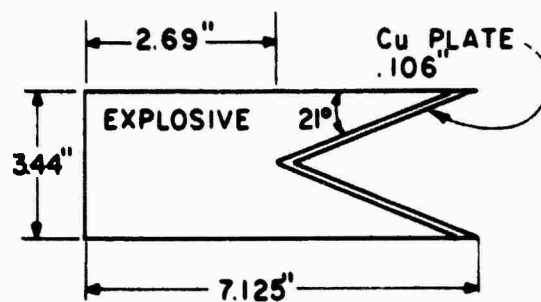


Fig 5

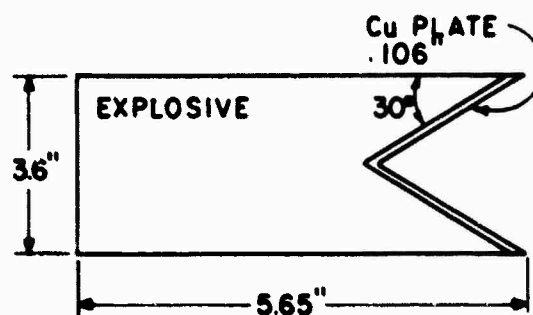


Fig 6

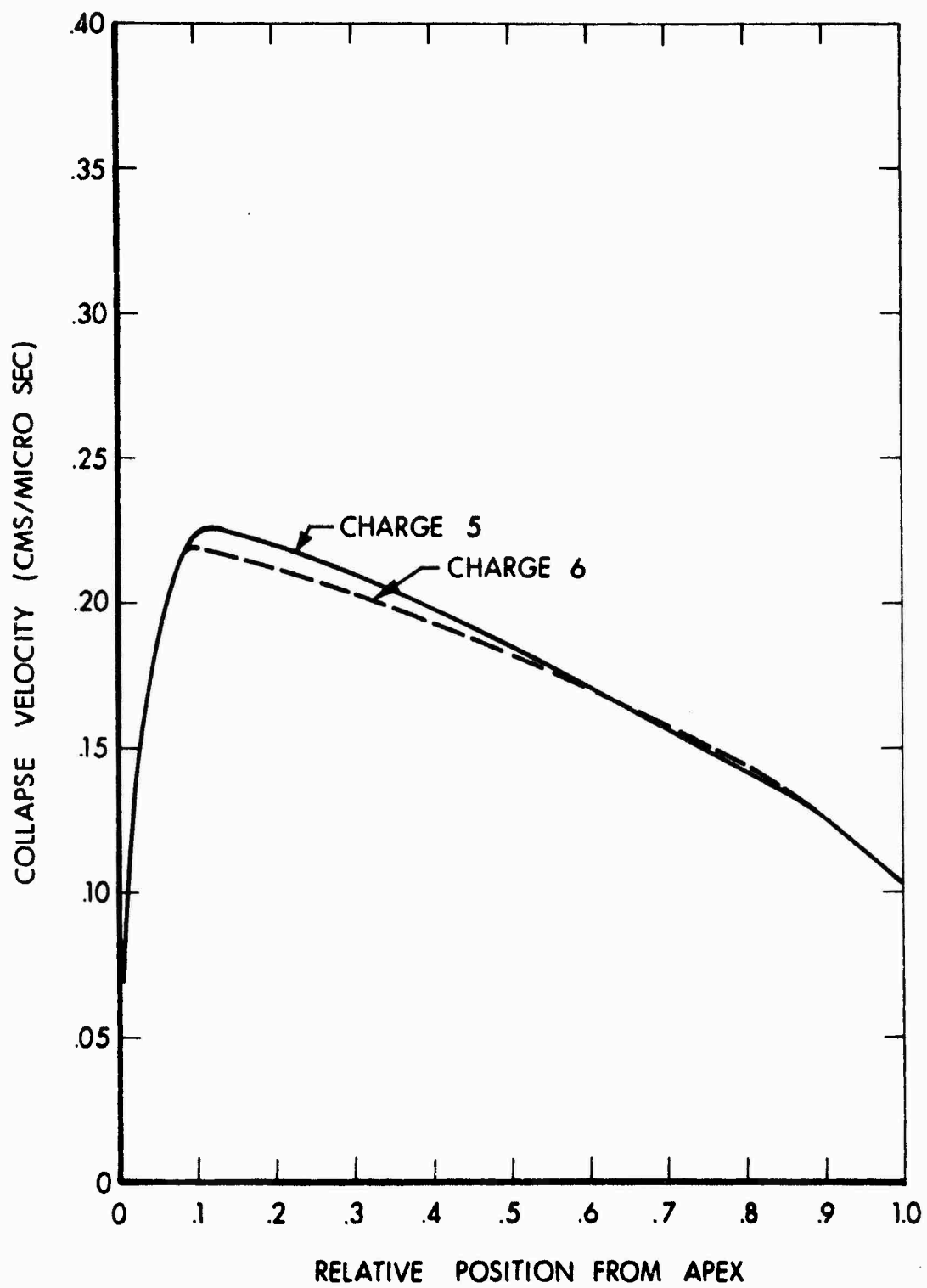


Figure 7

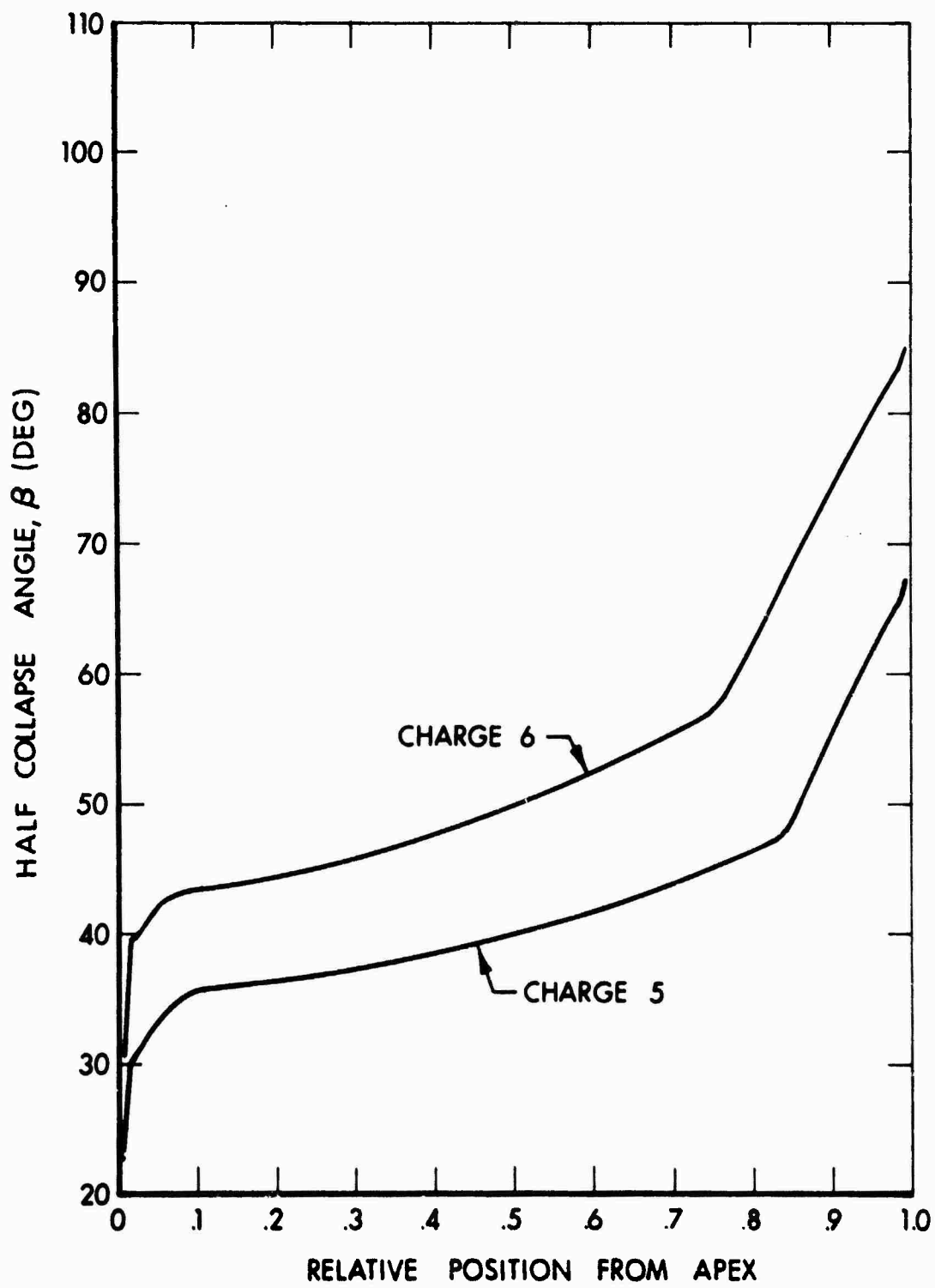


Figure 8



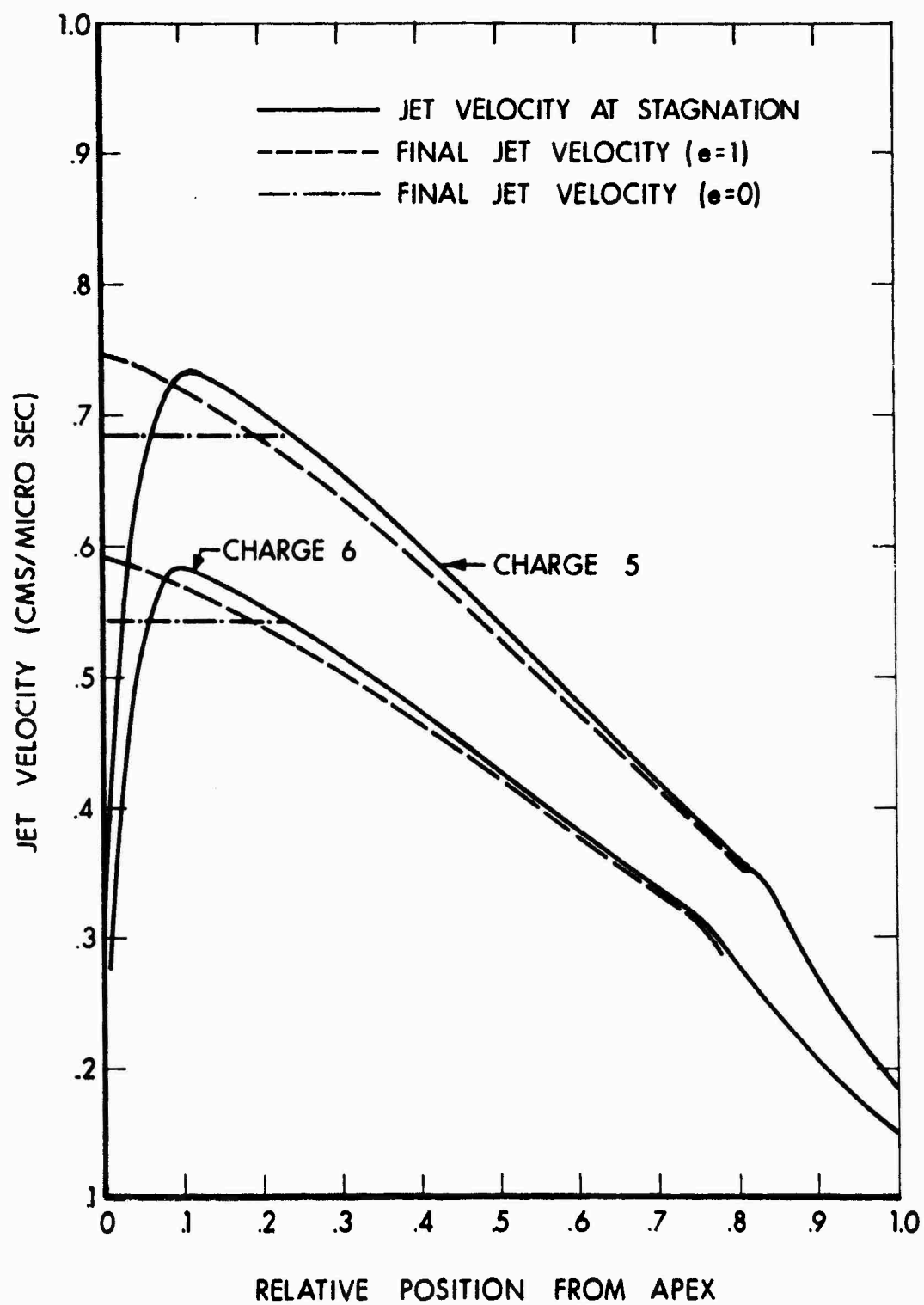


Figure 9

# DISTRIBUTION LIST

<u>No. of Copies</u>	<u>Organization</u>	<u>No. of Copies</u>	<u>Organization</u>
2	Commander Defense Documentation Center ATTN: TIPCR Cameron Station Alexandria, Virginia 22314	1	Commander U.S. Army Materiel Command ATTN: AMCRD-TC Washington, D.C. 20315
1	Director Advanced Research Projects Agency ATTN: Bal Msl Def/Rsch Div Department of Defense Washington, D.C. 20301	1	Commander U.S. Army Materiel Command ATTN: AMCRD-TP Washington, D.C. 20315
1	Director Institute for Defense Analyses 400 Army-Navy Drive Arlington, Virginia 22202	1	Commander U.S. Army Aviation Systems Command ATTN: AMSAV-E 12th & Spruce Streets St. Louis, Missouri 63166
1	Director Defense Nuclear Agency Washington, D.C. 20305	1	Director U.S. Army Air Mobility Research and Development Laboratory Ames Research Center Moffett Field, California 94035
1	Commander, Field Command Defense Nuclear Agency Sandia Base Albuquerque, New Mexico 87115	2	Commander U.S. Army Electronics Command ATTN: AMSEL-RD AMSEL-DL Fort Monmouth, New Jersey 07703
1	Commander U.S. Army Materiel Command ATTN: AMCDL Washington, D.C. 20315	4	Commander U.S. Army Missile Command ATTN: AMSMI-R AMSMI-XB AMSMI-RD Mr. J. Pettitt Dr. W. McCorkle Redstone Arsenal, Alabama 35809
1	Commander U.S. Army Materiel Command ATTN: AMCRD, Dr.J.V.R.Kaufman Washington, D.C. 20315		
1	Commander U.S. Army Materiel Command ATTN: AMCRD-TE Washington, D.C. 20315		

# DISTRIBUTION LIST

<u>No. of Copies</u>	<u>Organization</u>	<u>No. of Copies</u>	<u>Organization</u>
4	Commander U.S. Army Missile Command ATTN: AMSMI-RDI Mr. A. Poe, III Mr. E. Harwell, Jr. AMCPM-MW AMSMI-RBL Redstone Arsenal, Alabama 34809	1	PLASTEC U.S. Army Picatinny Arsenal ATTN: SMUPA-FR-M-D Dover, New Jersey 07801
2	Commander U.S. Army Tank-Automotive Command ATTN: AMSTA-RHFL AMSTA-B, Mr. A. Fisher Warren, Michigan 48090	6	Commander U.S. Army Picatinny Arsenal ATTN: SMUPA-D Mr. F. Saxe Mr. T. Stevens Mr. S. Jacobson Mr. R. Campoli (2 cys) Mr. W. Joseph Dover, New Jersey 07801
2	Commander U.S. Army Mobility Equipment Research & Development Center ATTN: Tech Docu Cen, Bldg. 315 AMSME-RZT Fort Belvoir, Virginia 22060	1	Commander U.S. Army Picatinny Arsenal ATTN: Mr. Glen Randers-Pehrson Dover, New Jersey 07801
1	Commander U.S. Army Munitions Command ATTN: AMSMU-RE Dover, New Jersey 07801	1	President U.S. Army Artillery Board Fort Sill, Oklahoma 73504
1	Commander U.S. Army Edgewood Arsenal ATTN: SMUEA-TSTI-L Edgewood Arsenal, Maryland 21010	1	President U.S. Army Infantry Board Fort Benning, Georgia 31905
3	Commander U.S. Army Frankford Arsenal ATTN: SMUFA-L7000 Mr. H. Markus Mr. H. George SMUFA-C2500 Philadelphia, Pennsylvania 19137	1	Commander U.S. Army Artic Test Center APO Seattle 98733
		2	Commander U.S. Army Weapons Command ATTN: AMSWE-RE AMSWE-RDF Rock Island, Illinois 61202
		1	Commander U.S. Army Rock Island Arsenal Rock Island, Illinois 61202
		1	Commander U.S. Army Watervliet Arsenal Watervliet, New York 12189

# DISTRIBUTION LIST

<u>No. of Copies</u>	<u>Organization</u>	<u>No. of Copies</u>	<u>Organization</u>
1	Director U.S. Army Advanced Materiel Concepts Agency 2461 Eisenhower Avenue Alexandria, Virginia 22314	1	Commander U.S. Army Combat Developments Command Experimentation Command Fort Ord, California 93941
1	Commander U.S. Army Harry Diamond Laboratories ATTN: AMXDO-TD/002 Washington, D.C. 20438	1	Commander U.S. Army Combat Developments Command Armor Agency Fort Knox, Kentucky 40121
4	Commander U.S. Army Materials and Mechanics Research Center ATTN: AMXMR-ATL AMXMR-XA Mr. K. Abbott AMXMR-XH Mr. J. Dignam AMXMR-P Watertown, Massachusetts 02172	1	Commander U.S. Army Combat Developments Command Field Artillery Agency Fort Sill, Oklahoma 73504
1	Commander U.S. Army Natick Laboratories ATTN: AMXRE, Dr. D. Sieling Natick, Massachusetts 01762	1	Commander U.S. Army Combat Developments Command Infantry Agency Fort Benning, Georgia 31905
3	Commander U.S. Army Combat Developments Command ATTN: CDCCG-SA, Mr.D.Hardison CDCMR-U CDCRE Fort Belvoir, Virginia 22060	1	Commander U.S. Army Artillery & Missile Center ATTN: AKPSIAS-G-RK Fort Sill, Oklahoma 73504
1	Commander U.S. Army Combat Developments Command Combat Arms Group Fort Leavenworth, Kansas 66027	1	Office of Vice Chief f Staff ATTN: CSAVCS-W-TIS Department of the Army Washington, D.C. 20310
		1	Chief of Engineers ATTN: ENGNF, Mine Warfare Br. Department of the Army Washington, D.C. 20315
		1	Chief of Research & Development Department of the Army Washington, D.C. 20310

# DISTRIBUTION LIST

<u>No. of Copies</u>	<u>Organization</u>	<u>No. of Copies</u>	<u>Organization</u>
1	Director U.S. Army Research Office 3045 Columbia Pike Arlington, Virginia 22204	1	Commander U.S. Naval Ship Research and Development Center ATTN: Code 753, Mr.A.Willner Washington, D.C. 20007
1	Commander U.S. Army Research Office (Durham) ATTN: CRD-AA-IPL Durham, North Carolina 27706	5	Commander U.S. Naval Weapons Center ATTN: Code 4561, Mr.R.Larson Code 40703, Mr.R.Sewell Code 603, Mr. J.Pearson Code 4560, Mr.P.Cordle Code 40701, Mr.M.Keith China Lake, California 93555
1	Department of Ordnance U.S. Military Academy ATTN: Assoc Prof West Point, New York 10996	1	Commander U.S. Naval Operations Test and Evaluation Force U.S. Naval Base Norfolk, Virginia 23511
1	Commandant U.S. Army War College Carlisle Barracks, Pennsylvania 17013	2	Commander U.S. Naval Ordnance Laboratory Silver Spring, Maryland 20910
1	Chief of Naval Operations ATTN: Prog Dev Div Department of the Navy Washington, D.C. 20350	1	Director U.S. Naval Research Laboratory Washington, D.C. 20390
3	Commander U.S. Naval Air Systems Command ATTN: AIR-604 Washington, D.C. 20360	1	Commander U.S. Naval Weapons Laboratory Dahlgren, Virginia 22448
3	Commander U.S. Naval Ordnance Systems Command ATTN: ORD-9132 Washington, D.C. 20360	1	Superintendent U.S. Naval Postgraduate School ATTN: Tech Repts Sec Monterey, California 93940
1	Commander U.S. Naval Air Development Center, Johnsville Warminster, Pennsylvania 18974	1	Commandant U.S. Marine Corps Washington, D.C. 20380
1	Commander U.S. Naval Missile Center Point Mugu, California 93041	3	AFATL (ATB; ATW; ATT) Eglin AFB Florida 32542

# DISTRIBUTION LIST

<u>No. of Copies</u>	<u>Organization</u>	<u>No. of Copies</u>	<u>Organization</u>
3	AFATL (DLRW, Mr. W. Dittrich) Eglin AFB Florida 32542	1	Director NASA Scientific & Technical Information Facility ATTN: SAK/DL P. O. Box 33 College Park, Maryland 20740
1	ADTC (ADBPS-12) Eglin AFB Florida 32542	1	Director John F. Kennedy Space Center, NASA ATTN: Tech Lib Kennedy Space Center, Florida 32899
1	AFWL (WLIL) Kirtland AFB New Mexico 87117	1	Director National Aeronautics and Space Administration Langley Research Center Langley Station Langley, Virginia 23365
1	AFML (MAY) Wright-Patterson AFB Ohio 45433	1	Director National Aeronautics and Space Administration Lewis Research Center 21000 Brookpark Road Cleveland, Ohio 44135
1	RTD (FDPE) Wright-Patterson AFB Ohio 45433	1	The Rand Corporation 1700 Main Street Santa Monica, California 90406
1	Science & Technology Division Library of Congress Washington, D.C. 20540	1	Drexel Institute of Technology Wave Propagation Research Center ATTN: Prof P. Chou 32nd & Chestnut Streets Philadelphia, Pennsylvania 19104
1	Director U.S. Bureau of Mines ATTN: Ch, Explo Rsch Lab 4800 Forbes Street Pittsburgh, Pennsylvania 15213	1	Director Applied Physics Laboratory The Johns Hopkins University ATTN: Mr. R. West 8621 Georgia Avenue Silver Spring, Maryland 20910
1	Headquarters U.S. Atomic Energy Commission ATTN: Tech Rept Lib Washington, D.C. 20545		
1	Director Lawrence Radiation Laboratory P. O. Box 808 Livermore, California 94550		
1	Director Los Alamos Scientific Laboratory P. O. Box 1663 Los Alamos, New Mexico 87544		

DISTRIBUTION LIST

<u>No. of</u> <u>Copies</u>	<u>Organization</u>
1	Stanford Research Institute Poulter Laboratories ATTN: Dr. G. Abrahamson 333 Ravenswood Avenue Menlo Park, California 94025

Aberdeen Proving Ground

Ch, Tech Lib  
Marine Corps Ln Ofc  
CDC Ln Ofc  
CG, USATECOM  
ATTN: AMSTE-BB

UNCLASSIFIED

Security Classification

DOCUMENT CONTROL DATA - R&D		
(Security classification of title, body of abstract and indexing annotation must be entered when the overall report is classified)		
1 ORIGINATING ACTIVITY (Corporate author)		2a REPORT SECURITY CLASSIFICATION
Ballistic Research Laboratories		Unclassified
Aberdeen Proving Ground, Maryland		2b GROUP
3 REPORT TITLE		
Theory And Computations Of Collapse And Jet Velocities Of Metallic Shaped Charge Liners		
4 DESCRIPTIVE NOTES (Type of report and inclusive dates)		
5 AUTHOR(S) (Last name, first name, initial)		
A. R. Kiwan and H. Wisniewski		
6 REPORT DATE	7a TOTAL NO. OF PAGES	7b NO. OF REFS
NOVEMBER 1972	38	9
8a CONTRACT OR GRANT NO.	9a. ORIGINATOR'S REPORT NUMBER(S)	
b PROJECT NO RDT&E 1T061102A33E	BRL REPORT NO. 1620	
c	9b. OTHER REPORT NO(S) (Any other numbers that may be assigned this report)	
d	" 7 FEB 1973	
10 AVAILABILITY LIMITATION NOTICES		
DISTRIBUTION LIMITED TO US GOVERNMENT AGENCIES ONLY. OTHER REQUESTS FOR THIS DOCUMENT MUST BE REFERRED TO DIRECTOR, USA BALLISTIC RESEARCH LABORATORIES, ATTN: AMXBR-XSE, ABERDEEN PROVING GROUND, MARYLAND 21005.		
11 SUPPLEMENTARY NOTES		12 SPONSORING MILITARY ACTIVITY
		U. S. Army Materiel Command Washington, D. C.
13 ABSTRACT		
<p>A model to compute the collapse velocities of various elements of a metallic liner of a shaped charge from the known detonation properties of the explosive used and the geometrical configurations of the charge is proposed. The calculated collapse and jet velocities increase from the apex of the liner toward the base, reach a maximum, and then decrease monotonically thereafter. The calculated velocity distribution in the jet after it goes through compression agrees qualitatively and quantitatively with available experimental measurements.</p>		



Unclassified  
Security Classification

14 KEY WORDS	LINK A		LINK B		LINK C	
	ROLE	WT	ROLE	WT	ROLE	WT
<p>Shape charge theory</p> <p>Detonation Theory, Mathematics, Numerical Analysis, Blast, Wave Propagation</p>						

**INSTRUCTIONS**

**1. ORIGINATING ACTIVITY:** Enter the name and address of the contractor, subcontractor, grantee, Department of Defense activity or other organization (*corporate author*) issuing the report.

**2a. REPORT SECURITY CLASSIFICATION:** Enter the overall security classification of the report. Indicate whether "Restricted Data" is included. Marking is to be in accordance with appropriate security regulations.

**2b. GROUP:** Automatic downgrading is specified in DoD Directive 5200.10 and Armed Forces Industrial Manual. Enter the group number. Also, when applicable, show that optional markings have been used for Group 3 and Group 4 as authorized.

**3. REPORT TITLE:** Enter the complete report title in all capital letters. Titles in all cases should be unclassified. If a meaningful title cannot be selected without classification, show title classification in all capitals in parenthesis immediately following the title.

**4. DESCRIPTIVE NOTES:** If appropriate, enter the type of report, e.g., interim, progress, summary, annual, or final. Give the inclusive dates when a specific reporting period is covered.

**5. AUTHOR(S):** Enter the name(s) of author(s) as shown on or in the report. Enter last name, first name, middle initial. If military, show rank and branch of service. The name of the principal author is an absolute minimum requirement.

**6. REPORT DATE:** Enter the date of the report as day, month, year; or month, year. If more than one date appears on the report, use date of publication.

**7a. TOTAL NUMBER OF PAGES:** The total page count should follow normal pagination procedures, i.e., enter the number of pages containing information.

**7b. NUMBER OF REFERENCES:** Enter the total number of references cited in the report.

**8a. CONTRACT OR GRANT NUMBER:** If appropriate, enter the applicable number of the contract or grant under which the report was written.

**8b, 8c, & 8d. PROJECT NUMBER:** Enter the appropriate military department identification, such as project number, subproject number, system numbers, task number, etc.

**9a. ORIGINATOR'S REPORT NUMBER(S):** Enter the official report number by which the document will be identified and controlled by the originating activity. This number must be unique to this report.

**9b. OTHER REPORT NUMBER(S):** If the report has been assigned any other report numbers (*either by the originator or by the sponsor*), also enter this number(s).

**10. AVAILABILITY/LIMITATION NOTICES:** Enter any limitations on further dissemination of the report, other than those imposed by security classification, using standard statements such as:

- (1) "Qualified requesters may obtain copies of this report from DDC."
- (2) "Foreign announcement and dissemination of this report by DDC is not authorized."
- (3) "U. S. Government agencies may obtain copies of this report directly from DDC. Other qualified DDC users shall request through \_\_\_\_\_."
- (4) "U. S. military agencies may obtain copies of this report directly from DDC. Other qualified users shall request through \_\_\_\_\_."
- (5) "All distribution of this report is controlled. Qualified DDC users shall request through \_\_\_\_\_."

If the report has been furnished to the Office of Technical Services, Department of Commerce, for sale to the public, indicate this fact and enter the price, if known.

**11. SUPPLEMENTARY NOTES:** Use for additional explanatory notes.

**12. SPONSORING MILITARY ACTIVITY:** Enter the name of the departmental project office or laboratory sponsoring (*paving for*) the research and development. Include address.

**13. ABSTRACT:** Enter an abstract giving a brief and factual summary of the document indicative of the report, even though it may also appear elsewhere in the body of the technical report. If additional space is required, a continuation sheet shall be attached.

It is highly desirable that the abstract of classified reports be unclassified. Each paragraph of the abstract shall end with an indication of the military security classification of the information in the paragraph, represented as (TS), (S), (C), or (U).

There is no limitation on the length of the abstract. However, the suggested length is from 150 to 225 words.

**14. KEY WORDS:** Key words are technically meaningful terms or short phrases that characterize a report and may be used as index entries for cataloging the report. Key words must be selected so that no security classification is required. Identifiers, such as equipment model designation, trade name, military project code name, geographic location, may be used as key words but will be followed by an indication of technical context. The assignment of links, rules, and weights is optional.